information

Article

A Proposal of the Fingerprint Optimization Method for the Fingerprint-Based Indoor Localization System with IEEE 802.15.4 Devices

Yuanzhi Huo [1], Pradini Puspitaningayu [1], Nobuo Funabiki [1,*], Kazushi Hamazaki [1], Minoru Kuribayashi [1] and Kazuyuki Kojima [2]

[1] Department of Electrical and Communication Engineering, Okayama University, Okayama 700-8530, Japan; pa9h1fz9@s.okayama-u.ac.jp (Y.H.); pradinip@s.okayama-u.ac.jp (P.P.); hamazaki4814@s.okayama-u.ac.jp (K.H.); kminoru@okayama-u.ac.jp (M.K.)
[2] Mechanical Engineering, Shonan Institute of Technology, Kanagawa 251-8511, Japan; kojima@mech.shonan-it.ac.jp
* Correspondence: funabiki@okayama-u.ac.jp

Abstract: Nowadays, human indoor localization services inside buildings or on underground streets are in strong demand for various location-based services. Since conventional GPS cannot be used, indoor localization systems using wireless technologies have been extensively studied. Previously, we studied a *fingerprint-based indoor localization system* using *IEEE802.15.4 devices*, called *FILS15.4*, to allow use of inexpensive, tiny, and long-life transmitters. However, due to the narrow channel band and the low transmission power, the *link quality indicator (LQI)* used for fingerprints easily fluctuates by human movements and other uncontrollable factors. To improve the localization accuracy, *FILS15.4* restricts the detection granularity to one room in the field, and adopts multiple fingerprints for one room, considering fluctuated signals, where their values must be properly adjusted. In this paper, we present a *fingerprint optimization method* for finding the proper fingerprint parameters in *FILS15.4* by extending the existing one. As the *training* phase using the measurement LQI, it iteratively changes fingerprint values to maximize the newly defined *score function* for the room detecting accuracy. Moreover, it automatically increases the number of fingerprints for a room if the accuracy is not sufficient. For evaluations, we applied the proposed method to the measured LQI data using the *FILS15.4* testbed system in the no. 2 Engineering Building at Okayama University. The *validation* results show that it improves the average detection accuracy (at higher than 97%) by automatically increasing the number of fingerprints and optimizing the values.

Keywords: indoor localization; fingerprint; IEEE802.15.4; LQI; parameter optimization

Citation: Huo, Y.; Puspitaningayu, P.; Funabiki, N.; Hamazaki, K.; Kuribayashi, M.; Kojima, K. A Proposal of the Fingerprint Optimization Method for the Fingerprint-Based Indoor Localization System with IEEE 802.15.4 Devices. *Information* **2022**, *13*, 211. https://doi.org/10.3390/info13050211

Academic Editors: Chih-Peng Fan, Konstantinos E. Psannis, Muh-Tian Shiue, Hsi-Pin Ma and Abderrezak Rachedi

Received: 24 February 2022
Accepted: 16 April 2022
Published: 20 April 2022

1. Introduction

Currently, a variety of location-based services have been offered in outdoor and indoor environments. While the *global positioning system (GPS)* can be used for outdoors, it fails to cover indoor fields [1,2]. Then, to cover indoors, *indoor localization systems* have been explored using different wireless technologies, such as *RFID*, *ultra wide-band (UWB)*, *IEEE 802.11 Wi-Fi*, and *Bluetooth* [3], and various positioning techniques [4], such as *fingerprinting*, *time difference of arrival (TDoA)*, *angle of arrival (AoA)*, *lateration*, *pattern matching*, etc.

Fingerprinting has gained great interest due to the capability of achieving reasonable accuracy using the *radio map pattern matching* [5]. This method consists of the *calibration phase* and the *detection phase*. In the *calibration phase*, the *radio signal map* for each location or section in the target field is collected and stored, assuming that each section has its own specific radio pattern called the *fingerprint*, which should be different from the one in another section. In the *detection phase*, the radio signal is compared with each fingerprint in the radio map, and the closest one is selected to identify the current location. With considerable calibration efforts, this method can provide robust detection capabilities [6].

Previously, we developed a *fingerprint-based indoor localization system* using the *IEEE802.15.4* protocol, called *FILS15.4* for convenience [7,8]. *FILS15.4* adopts *IEEE802.15.4* devices from *Mono Wireless* [9], because the transmitter is inexpensive (30US), tiny (13.97 $\times$ 13.97 $\times$ 2.5 mm, 0.93 g), has long-life, no user software to download, and no user setup; it is suitable to be always be worn by a user during location detection. The signal from the transmitter can be received at multiple receivers that are fixed in the field at the same time. When the transmitter is located at a specific location, the *LQI (link quality indicator)* at the receiver becomes the fingerprint to the location.

However, the LQI of this device can be easily fluctuated due to human movements in the field and transmission environment changes from opening/closing doors and other wireless signals at the 2.4 GHz band, because of the small transmission power and the narrow channel bandwidth of *IEEE802.15.4*. This *signal fluctuation problem* can cause the misdetection of *FILS15.4* and becomes the bottleneck of using this device for the *indoor localization system*.

For many practical applications and services for *indoor localization systems*, it will be sufficient to detect the room in a building where the user is currently staying, instead of the exact coordinate of the user location. Then, if a room is regarded as the least localization unit, the signal fluctuation problem may be overcome. Since walls separating rooms in the field attenuate the wireless signal sufficiently, the signal strength in the room can be different from the ones in other rooms, where the difference can be larger than the fluctuation range.

By limiting the detection granularity to one room, it is expected to achieve high accuracy, even using *IEEE802.15.4* devices. Moreover, it becomes possible to use plural fingerprints with different values to represent one room. Therefore, *FILS15.4* has been designed to detect the 'currently staying room' of a user and to adopt multiple fingerprints for each room detection. Then, it becomes critical to optimize the number of fingerprints for each room and the fingerprint values, which will be hard if done manually.

In this paper, we present the *fingerprint optimization method* for *FILS15.4* to automatically optimize the number of fingerprints and their values for every room, by employing the existing parameter optimization tool in [10]. The procedure of calculating the *score* to evaluate the optimality of the current fingerprint selection is newly defined to determine the validity of the parameter changes in the method. For the given measured data sets where the correct detection results are known, this method automatically changes the number of fingerprints and their values to maximize the *score*.

For evaluations, we applied the proposed method to the measured LQI data at the no. 2 Engineering Building at Okayama University. The results show that the average detection accuracy rises higher than 97% for any room by increasing the number of fingerprints and setting the proper values by the method. Moreover, the results with the transmitter, under LQI fluctuation causes, also showed high accuracy using the same set of fingerprints.

The rest of this paper is organized as follows: Section 2 presents comparisons of various localization techniques of indoor localization systems. Section 3 reviews *FILS15.4* and discusses the LQI fluctuation problem. Section 4 presents the fingerprint optimization method for *FILS15.4*. Sections 5 and 6 show the evaluations of the proposal in the detection accuracy of static LQI data and detection accuracy over time. Section 7 shows the evaluations with fluctuation causes. Section 8 presents evaluation results by using the proposed method. Section 9 shows the related work. Section 10 concludes this paper with future works.

2. Comparison of Indoor Localization Techniques

In this section, we compare the features of typical indoor localization techniques.

We compared the features of the four typical indoor localization techniques, namely, *fingerprinting* in the proposal, *signal propagation model-based method*, *time of arrival (ToA)*, and *angle of arrival (AoA)*, in Table 1.

Table 1. Comparison of indoor localization techniques.

Feature	Fingerprinting	Signal Propagation Model-Based	Time of Arrival (ToA)	Angle of Arrival (AoA)
accuracy	high	low	high	low
time synchronization	no	no	yes	no
directional antenna	no	no	no	yes
implementation cost	low	low	high	high

The *signal propagation model-based method* needs the mathematical model to accurately estimate the RSS at every necessary location in the indoor environment. However, the required accurate model may not exist because the signal attenuations by various obstacles or materials are hard to estimate. The RSS is often affected by environmental changes such as human movements, door opening/closing, and other interfering wireless signals, and even temperature/moisture changes. Therefore, this method suffers from low accuracy.

ToA needs the accurate time synchronization between the transmitter and the receiver, because the distance between them is calculated by the difference between the radio signal transmission time at the transmitter and its reception time at the receiver. This requirement increases the implementation cost.

AoA needs the accurate detection of the signal reception angle from the transmitter using the accurate directional antenna. However, conventional user devices, such as personal computers and smartphones, are not equipped with such antennas. Thus, this requirement also increases the implementation cost.

On the other hand, *fingerprinting* does not need such special hardware or software and can reduce the implementation cost. References in [11,12] show that this method gives robust accuracy by building the radio map of the known locations in the target field by collecting the received signal strength information under various environmental changes. Therefore, we chose the fingerprinting method as the indoor localization technique in this paper.

Furthermore, in *FILS15.4*, multiple signal strengths under different propagations, which are necessary in location detections, are obtained by receiving the wireless signal from one transmitter attached to the user, at the multiple receivers that are fixed at different locations in the field. On the other hand, in Wi-Fi-based systems, they are obtained by receiving the signals from different transmitters (access points), at the receiver that is attached to the user and can be often moved. *FILS15.4* can send the received signal information to the server without using the mobile communication system, which can reduce the operation cost and enhance the dependability.

3. Review of *FILS15.4* and the Fluctuation Problem

In this section, we review *FILS15.4* and the signal fluctuation problem in our previous works.

3.1. System Overview

Figure 1 shows the system overview of *FILS15.4*. The user carries the transmitter during detections. The transmitter transmits the data at the 500 ms interval to the receivers that are located at the fixed locations in the field and are attached to *Raspberry Pi* devices by USB connections. The received data and LQI are sent to the server using the MQTT protocol system at the 60 s interval. The server compares the received LQI with the stored fingerprints and finds the current room of the user.

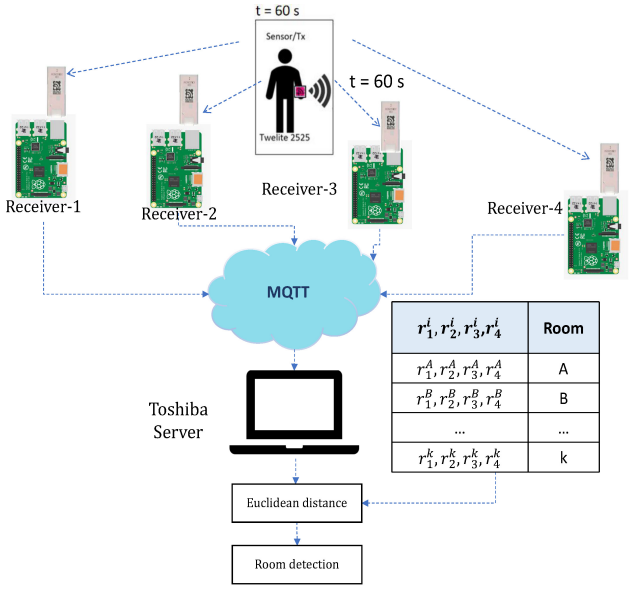

Figure 1. *FILS15.4* system overview.

3.2. IEEE 802.15.4 Devices

In *FILS15.4*, the devices following the *IEEE 802.15.4* standard from *Mono Wireless* [9] were adopted. For the transmitter, *Twelite 2525* was used. The size of this transmitter was only 2.5 $\times$ 2.5 $\times$ 1 cm, which is suitable to be carried by the user. During our experiments, it was attached on the wrist of the user. This device uses the 2.4 GHz band, which can be interfered with *IEEE 802.11 Wi-Fi*.

For the receiver, *Mono Stick* was used and was connected to *Raspberry Pi* over a USB port. *Raspberry Pi* receives the packets from the transmitter and monitors the *link quality indication (LQI)* at the packet reception. Then, every one minute, it transmits the data in the packets and the LQI data to the server through the *MQTT protocol* [13].

The server stores the received data in the *SQLite* database, calculates the average LQI, combines the values from all the receivers as a vector, saves them as the fingerprint with the corresponding location label in the *calibration phase*, or calculates the Euclidean distance between the measured average LQI and each fingerprint to detect the current room in the *detection phase*.

3.3. Calibration Phase

In the *calibration phase*, the server calculates the fingerprint for each room offline by the following procedure. The calibration phase flow chart shows in Figure 2:

(1) Properly locate the *Raspberry Pi* devices with the receivers in the target field.
(2) Run the programs and create the connection to the MQTT broker.
(3) Locate the transmitter at the specified location in the field. In our experiments, we selected 18 locations where we moved the transmitter from one place to another after measuring LQI for one minute by transmitting packets every 500 ms.
(4) Receive and collect the packets from the transmitter at the *Raspberry Pi* device for one minute.
(5) Forward the collected data from the *Raspberry Pi* device to the server through the MQTT broker.
(6) For each receiver, calculate the average LQI using the forwarded data from it after the last average LQI calculation.
(7) Make the fingerprint at the server, and store them in the SQLite database.

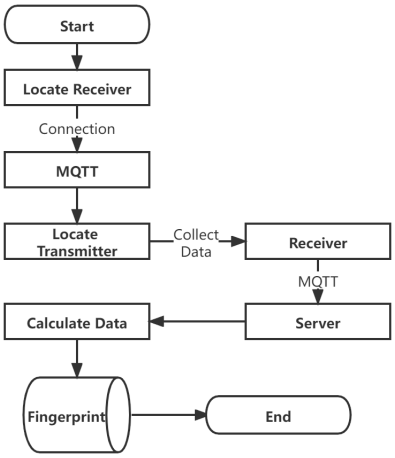

Figure 2. Calibration phase flow chart.

3.4. Detection Phase

In the *detection phase*, the server detects the current room of the user by applying steps (1)–(6) in the procedure for the *calibration phase* periodically. Then, in step (7), after the vector of the average LQI values from all the receivers are obtained, the Euclidean distance is calculated against every pre-stored fingerprint by Equation (1), and the room whose fingerprint has the smallest distance is appointed as the detected room.

$$disF_i^k = \sqrt{\sum_{j=1}^{n}(r_j^i - R_j^k)^2} \tag{1}$$

where

- $disF_i^k$ represents the Euclidean distance between the i-th measured average LQI and the fingerprint for room k;
- r_j^i does the i-th measured average LQI at receiver j; and
- R_j^k does a fingerprint for room k at receiver j.

3.5. Signal Fluctuation Problem

In our preliminary experiments, we collected LQI data for one hour using five receivers on the third floor of the no. 2 Engineering Building at Okayama University in Figure 3 and observed the signal fluctuation problem.

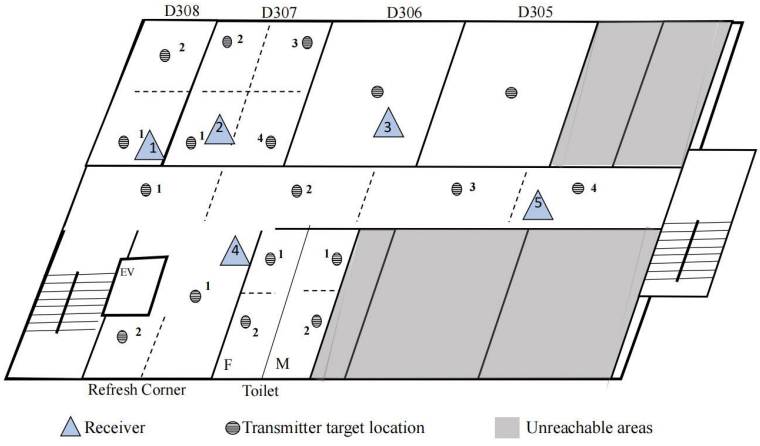

Figure 3. Experiment field layout for fluctuations causes.

Figure 4 shows the measured LQI data at the five receivers, *LQ1–LQ5*, when the transmitter was located at *D307-2*. Any data always fluctuated. Sometimes no data were received at the four receivers except *LQ2* due to the *connection loss*, where $LQI = 5$ indicates no data reception. It could be caused by the human movements in the field, where someone in the field. blocked the signal path, or closed the door of the room.

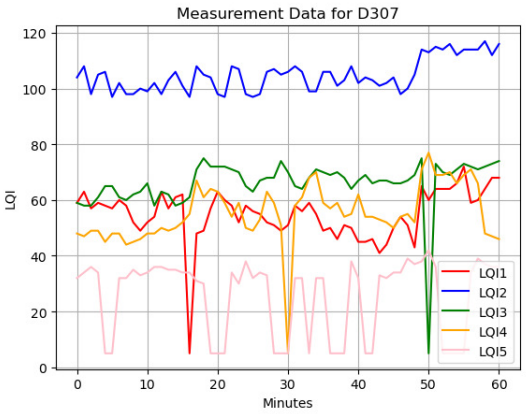

Figure 4. Measured LQI data for *D307-2*.

3.6. LQI Observations

Let us discuss the observations of each LQI data in Figure 4.

- At *LQ2*, which comes from the nearest receiver from the transmitter, no *connection loss* appeared, and two different LQI levels can be observed.
- At *LQ1*, *LQ3*, and *LQ4*, one *connection loss* appeared, and two-three different LQI levels can be observed.
- At *LQ5*, *connection loss* often appeared, whereas the LQI level is almost constant.

These observations suggest that the plural fingerprints are necessary for this room where the number and their values should be properly selected based on the data.

4. Fingerprint Optimization Method for *FILS15.4*

In this section, we present the fingerprint optimization method for *FILS15.4* by extending the work in [10].

4.1. Parameter Symbols

First, we define the parameter symbols to present the procedure of the fingerprint optimization method.

- P: the set of the n parameters for the algorithm/logic in the logic program whose values should be optimized. In this paper, each parameter represents one fingerprint value.
- p_i: the value of the ith parameter (fingerprint) in P ($1 \leq i \leq n$).
- p_i^{init}: the initial value of the ith parameter in P ($1 \leq i \leq n$).
- Δp_i: the change step for p_i.
- t_i: the tabu period for p_i in the tabu table.
- $S(P)$: the score of the algorithm/logic using P.
- P_{best}: the best set of the parameters.
- $S(P_{best})$: the score of the algorithm/logic where P_{best} is used.
- L: the log of the generated parameter values and their scores.
- M: the number of rooms in the field.
- R: the number of receivers.
- F_j^k:the j-th fingerprint vector for the k-th room ($1 \leq k \leq M$).

- ft_k: the number of trials for fingerprint number optimization for the k-th room ($1 \leq k \leq M$).
- FT: the maximum number of trials for fingerprint number optimization.

Among them, Δp_i, t_i and FT need to be properly set as the algorithm parameters in the proposal. Actually, in this paper, $\Delta p_i = 1$, $t_i = 10$, and $FT = 3$ are used.

4.2. Algorithm Procedure

The proposed parameter optimization method consists of three phases. The following procedure describes it for optimizing the parameter values in P to minimize the score $S(P)$:

Initialization Phase

(1) Clear the generated parameter log L.
(2) Initialize the number of fingerprint increase trials for the k-th room by: $ft_k = 0$ ($1 \leq k \leq M$).
(3) Set the initial value in the parameter file for any p_i in P, set 0 for any tabu period t_i, and set a large value for $S(P_{best})$.

Fingerprint Value Optimization Phase

(4) Generate the neighborhood parameter value sets for P by:
  (a) Randomly selecting one parameter p_i for $t_i = 0$.
  (b) Calculate the parameter values of ${p_i}^-$ and ${p_i}^+$ by:

$$\begin{aligned} {p_i}^- &= p_i - \Delta p_i, \text{if } p_i > \text{lower limit}, \\ {p_i}^+ &= p_i + \Delta p_i, \text{if } p_i < \text{upper limit}. \end{aligned} \tag{2}$$

  (c) Generate the neighborhood parameter value sets P^- and P^+ by replacing p_i by ${p_i}^-$ or ${p_i}^+$:

$$\begin{aligned} P^- &= \{p_1, p_2, \ldots, {p_i}^-, \ldots, p_n\} \\ P^+ &= \{p_1, p_2, \ldots, {p_i}^+, \ldots, p_n\} \end{aligned}$$

(5) When P (P^-, P^+) exists in L, obtain $S(P)$ ($S(P^-)$, $S(P^+)$) from L. Otherwise, execute the logic program using P (P^-, P^+) to obtain $S(P)$ ($S(P^-)$, $S(P^+)$), and write P and $S(P)$ (P^- and $S(P^-)$, P^+ and $S(P^+)$) into L.
(6) Compare $S(P)$, $S(P^-)$, and $S(P^+)$, and select the parameter value set that has the largest one among them.
(7) Update the tabu period by:
  (a) Decrement t_i by -1 if $t_i > 0$.
  (b) Set the given constant tabu period TB for t_i if $S(P)$ is the largest at (6) and p_i is selected at (4)(a).
(8) When $S(P)$ is continuously largest at (6) for the given constant times, go to (9). Otherwise, go to (4).
(9) When the hill-climbing procedure in (10) is applied for the given constant times HT, go to (11) as the state is converged. Otherwise, go to (10).
(10) Apply the hill-climbing procedure:
  (a) If $S(P) < S(P_{best})$, update P_{best} and $S(P_{best})$ by P and $S(P)$.
  (b) Reset P by P_{best}.
  (c) Randomly select p_i in P, and randomly change the value of p_i within its range and go to (4).
(11) Terminate the algorithm and output the current fingerprint parameter values if the number of fingerprint increase trials for every room become the maximum: $ft_k = FT$.

Fingerprint Number Optimization Phase

(12) If the last fingerprint increase (the k-th room) cannot improve the score function $S(P_{best})$, increment ft_k by 1, and rollback the previous fingerprint parameter values before this last fingerprint increase.
(13) Save and keep the current fingerprint parameter values for the rollback procedure.
(14) Randomly select one room (let the k-th room) that has $ft_k < FT$ (which does not reach the maximum trials).
(15) Generate a new fingerprint for the k-th room by increasing n to n+R and by copying the parameter value of a randomly selected fingerprint for the same k-th room. Here, each of the R parameter values for the new fingerprint is copied from the corresponding parameter value of the randomly selected fingerprint for the same room.
(16) Set 0 for the tabu period t_i of any fingerprint parameter, and set a large value for $S(P_{best})$.
(17) Go to (4).

Initialization phase describes the procedure of initializing the necessary variables in the method. **Fingerprint value optimization phase** describes the procedure of optimizing the fingerprint values when the number of fingerprints for each room is fixed. **Fingerprint number optimization phase** describes the procedure of optimizing the number of fingerprints for each room, which is newly presented in this paper.

4.3. Score Calculation Procedure

The procedure of calculating the score $S(P)$ for a given set of fingerprint values P and the measured LQI is presented as follows:

(1) Calculate the Euclidean distance $disF_i^k$ between the i-th average measured LQI and the k-th current fingerprint.
(2) Find $disF^{OK}$ that represents the minimum Euclidean distance against a fingerprint representing the correct room.
(3) Find $disF^{NG}$ that represents the minimum Euclidean distance against a fingerprint representing the incorrect room.
(4) Calculate $S(P)$ by:

$$S(P) = A\sum_{i=1}^{N} true(disF^{OK} - disF^{NG}) + B\sum_{i=1}^{N}\frac{disF^{NG}}{disF^{OK}} + C\sum_{k=1}^{M}\underset{b\neq c}{min} \mid F_b^k - F_c^k \mid \quad (3)$$

where A and B represent constant coefficients ($A = 10$, $B = 1$ and $C = 1$ in this paper), N is the number of the average measured LQI for the optimization, the function $true(x)$ returns 1 if $x > 0$ and 0 otherwise. The C-term represents the sum of the minimum Euclidean distance between two different fingerprints for the same room. It intends to generate different fingerprint values for the same room. Optimization method flow in Figure 5.

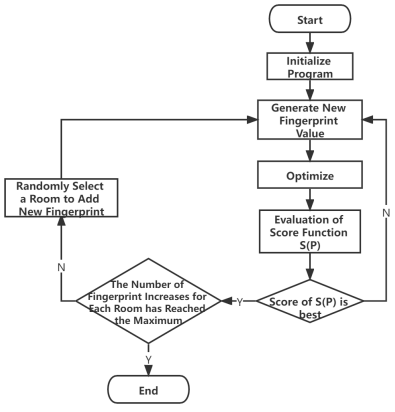

Figure 5. Fingerprint optimization method flow chart.

5. Evaluation of Detection Accuracy

In this section, we evaluate the proposal in terms of the detection accuracy using the measured LQI data by *FILS15.4* on the third floor of the no. 2 Engineering Building at Okayama University in Figure 3.

5.1. Field Layout

This field was composed of six rooms and one corridor. Five receivers were deployed to be balanced between them. The transmitter was moved to each transmitter target location and was kept running for one week to collect measured LQI data at each location.

5.2. Detection Result before Proposal

First, we discuss the detection results before applying the proposal.

5.2.1. Fingerprints

Here, we prepared one fingerprint for each room and selected the values by taking the average of the measured LQI data. Table 2 shows the fingerprint values for the seven rooms including the corridor.

Table 2. Fingerprint before proposal.

Room	R_1^k	R_2^k	R_3^k	R_4^k	R_5^k
RC	74	33	14	147	22
Corridor	38	46	68	36	112
D306	29	15	118	41	53
D307	65	112	48	50	10
D308	81	77	30	66	5
Toilet	62	5	66	49	52
D305	5	5	37	34	59

5.2.2. Detection Results

Table 2 shows the results by *FILS15.4* before applying the proposal, when each room is assigned one fingerprint. This table includes the room detection accuracy, the average of the minimum distance to the correct room ($disF^{OK}$), the average of the minimum distance to incorrect room ($disF^{NG}$), and the difference between $disF^{NG}$ and $disF^{OK}$ (*margin*). The detection accuracy is calculated by $(total\_time - misdetection\_time)/total\_time \times 100$, where $total\_time$ represents the total time of measuring the LQI data, and $misdetection\_time$ does the sum of the time of incorrectly detecting the room among them.

The detection accuracy at *Toilet* is lowest and that at the *corridor* is the next, which is less than 80%. For them, the *margin* is very small compared with the others. Thus, even small fluctuations of LQI can cause misdetections for them. When the score $S(P)$ in Equation (3) is calculated, it becomes 201,407.64, which should be improved.

5.3. Detection Result after Proposal

Then, we applied the proposed method by using the fingerprint values in Table 3 for the initial parameter values. For this application, we divided the collected LQI data of the seven days into two sets. The first set contained the LQI data of the four days that were used to optimize the fingerprints using the proposed method for *training*. The second set contained the LQI data of the remaining three days used to validate the detection accuracy by the optimized fingerprints for *validation*. Meanwhile, we trained the classification ANN model by using same data to compare detection accuracy with our proposed method. The model structure of ANN is shown as Figure 6.

Table 3. Room detection results before proposal.

Room	Accuracy	$disF^{OK}$	$disF^{NG}$	Margin
RC	99.34%	41.03	93.05	52.02
Corridor	87.4%	81.58	86.32	4.74
D306	98.28%	54.14	80.43	26.29
D307	92.51%	52.28	74.84	22.56
D308	90.32%	39.44	61.44	22
Toilet	76.96%	49.37	63.56	14.19
D305	100%	31.23	61.72	30.49
Average	92.12%	49.87	74.48	24.61

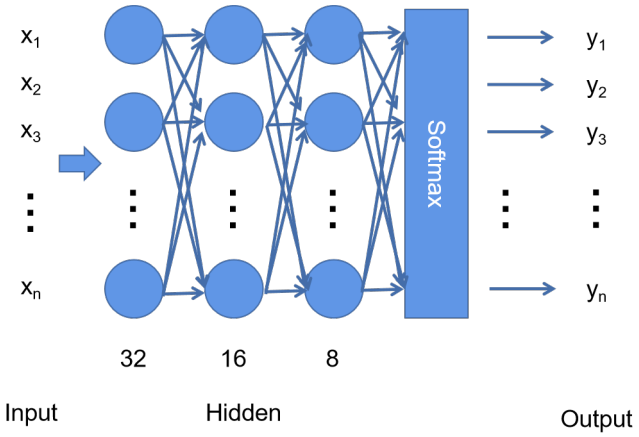

Figure 6. ANN model structure.

5.3.1. Fingerprints

Table 4 shows the fingerprint values that are obtained by applying the proposal to the four-day training data set. In this table, three fingerprints were automatically generated for the *corridor* and *toilet* by the proposal, because they were either long or had several small rooms, and people often moved there. Two fingerprints were generated for *RC*, *D307*, *D308*, and *D305*, because people sometimes moved there and there were several pieces of furniture. For *D306*, it kept one fingerprint, because only a few people moved into this meeting room.

Table 4. Fingerprint after proposal.

Room	R_1^k	R_2^k	R_3^k	R_4^k	R_5^k
RC-1	66	40	30	130	26
RC-2	7	24	37	139	5
Corridor-1	12	22	30	64	98
Corridor-2	118	48	26	70	93
Corridor-3	23	40	67	26	116
D306	24	31	124	45	40
D307-1	39	5	70	83	14
D307-2	68	112	48	50	22
D308-1	79	78	30	66	8
D308-2	99	5	10	43	9
Toilet-1	62	15	46	41	52
Toilet-2	42	5	46	60	21
Toilet-3	5	5	34	30	50
D305-1	159	60	97	6	26
D305-2	5	5	37	34	59

5.3.2. Detection Results

Tables 5 and 6 show the room detection results by using the optimized fingerprints by the proposal for the training data set and for the validation data set, respectively, and detection results of the ANN model. The score is 161,762.58 for the training data set and is 53,503.53 for the validation data set. Thus, the total score is 215,266.11.

Table 5 indicates that the detection accuracy exceeds 98% for any room by using the LQI data set for training, whether it is the proposed method or ANN. The average detection accuracy of the proposed method higher than ANN model. Then, Table 6 indicates that the detection accuracy exceeds 98% for any room except for *D306* by using the proposed method, although the LQI data set is different from the one for training. For this room, the proposal did not increase the number of fingerprints, which can be a reason for this low accuracy. The detection accuracy of the ANN model is lower than our proposed method, especially just 90.7% for *D308*. In future works, we will analyze the reason and study how to improve it. The room detection results using the validation data set confirms the effectiveness of the proposal. Figures 7 and 8 show the comparison of detection accuracy. Figures 9–12 show the CDF graph and confusion matrix of detection accuracy for training LQI data and validation LQI data by using proposed method.

Table 5. Room detection result for training data.

Room	Accuracy (POT)	Accuracy (ANN)	$disF^{OK}$	$disF^{NG}$	Margin
RC	99.1%	99.6%	40.21	88.53	48.32
Corridor	99.3%	99.3%	55.96	80.13	24.17
D306	99.2%	99.2%	50.47	85.71	35.24
D307	99.5%	99.2%	46.58	78.00	31.42
D308	98.4%	99%	35.10	59.89	24.79
Toilet	98.8%	98.7%	40.96	57.32	16.36
D305	99.9%	98.3%	26.86	35.31	8.45
Average	99.2%	99%	42.31	69.27	26.96

Table 6. Room detection result for validation data.

Room	Accuracy (POT)	Accuracy (ANN)	$disF^{OK}$	$disF^{NG}$	Margin
RC	100%	99.9%	46.42	68.70	22.28
Corridor	98.6%	97.9%	73.74	80.80	7.06
D306	95.2%	93.6%	45.88	83.09	37.21
D307	98.5%	94.5%	30.46	50.84	20.38
D308	98.8%	90.7%	34.11	64.37	30.26
Toilet	98.4%	95.5%	29.72	46.01	16.29
D305	100%	98.9%	44.20	48.53	4.33
Average	98.5%	95.9%	43.50	63.19	19.69

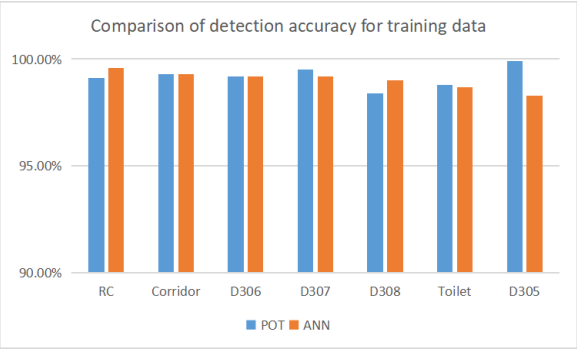

Figure 7. Comparison of detection accuracy for training data.

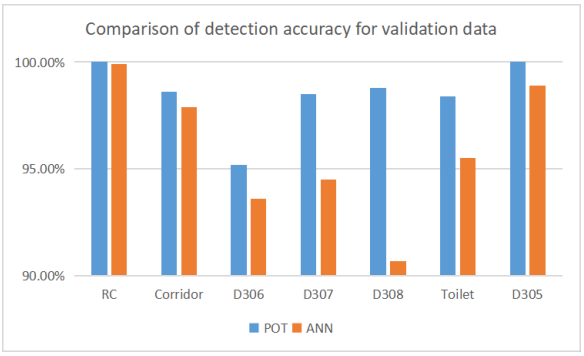

Figure 8. Comparison of detection accuracy for validation data.

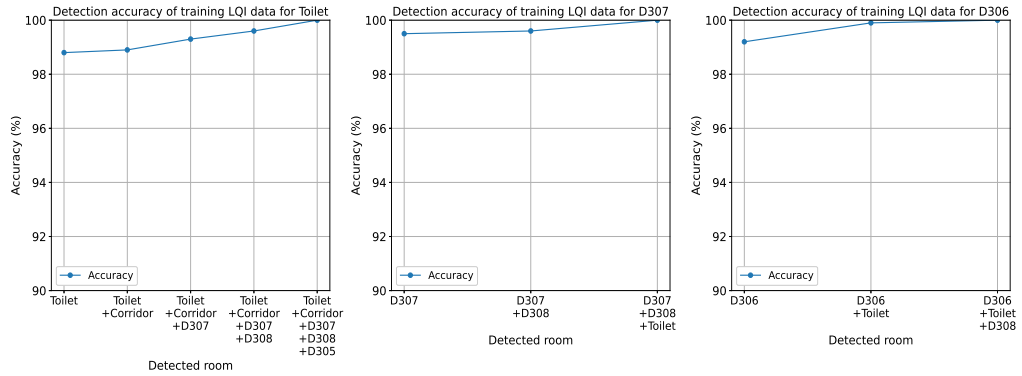

Figure 9. CDF graph of detection accuracy for training LQI data.

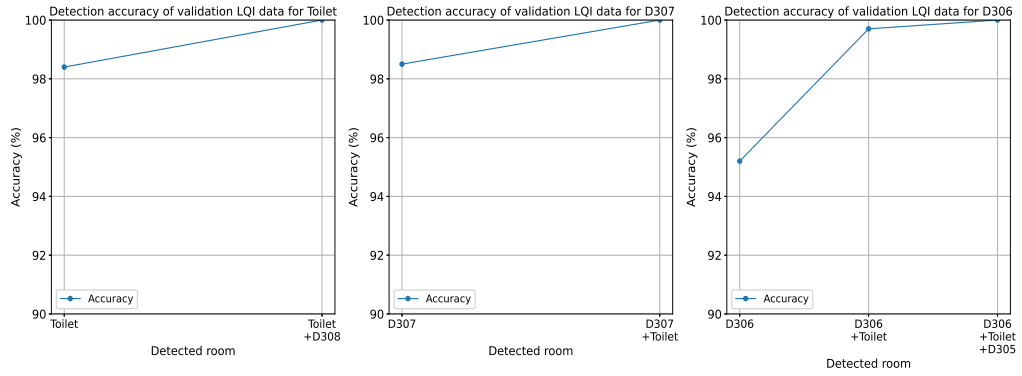

Figure 10. CDF graph of detection accuracy for validation LQI data.

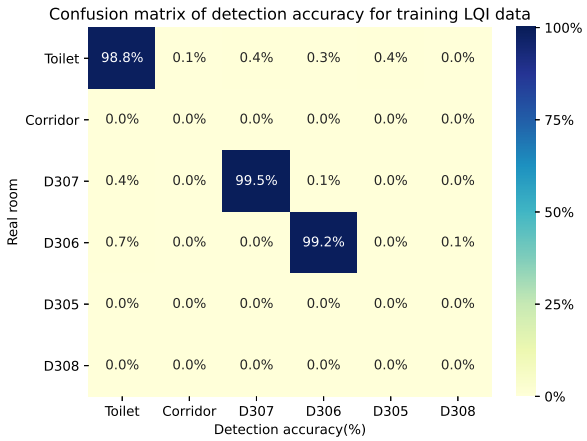

Figure 11. Confusion matrix of detection accuracy for training LQI data.

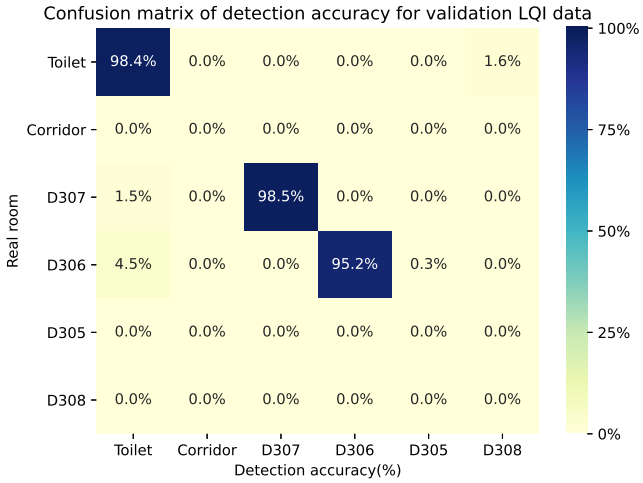

Figure 12. Confusion matrix of detection accuracy for validation LQI data.

5.4. Measured LQI Data and Detection Result for Toilet

Tables 5 and 6 show that the detection rate of *Toilet* is most improved by the proposal, from 76.96% to 98.8% for training data and 98.4% for validation data. Figures 13 and 14 show the training LQI data set and the validation LQI data set for *Toilet*, respectively. In both data sets, the measured LQI data at any receiver often fluctuated, where students sometimes walked through the *corridor* and entered the *toilet*. Thus, the proposal increased the number of fingerprints to three. Tables 7 and 8 show the details of the room detection results for them, where the *corridor*, *D307*, *D308*, and *D305* are incorrectly detected instead of the *toilet*.

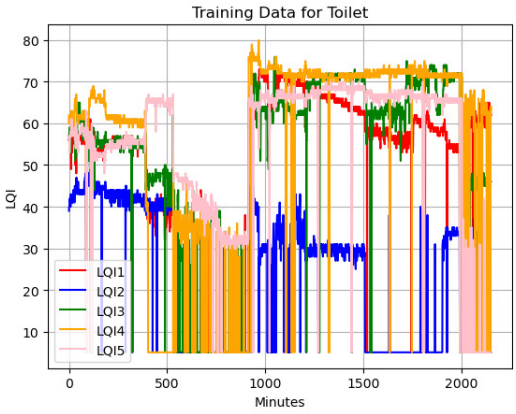

Figure 13. Training LQI data set for *toilet*.

Table 7. Room detection results for training data of the *toilet*.

Room	Periods (min)	Percentage
Toilet	1∼88, 90∼91, 93∼117, 121∼936, 938, 940∼1106, 1108∼1270, 1273∼1274, 1276∼1439, 1441∼1518, 1520∼1538, 1540∼1633, 1636∼1743, 1745∼1802, 1804, 1806∼1809, 1811∼1813, 1815∼1925, 1927∼2037, 2039∼2040, 2042∼2097, 2099∼2150	98.8%
Corridor	1275, 1539	0.1%
D307	937, 939, 1271∼1272, 1440, 1803, 1805, 1810	0.4%
D308	92, 118∼120, 2038, 2041, 2098	0.3%
D305	89, 1107, 1519, 1634∼1635, 1744, 1814, 1926	0.4%

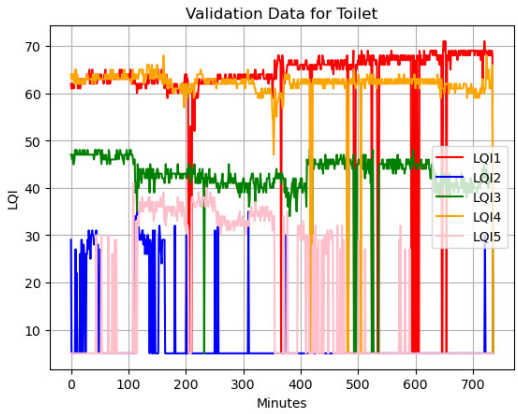

Figure 14. Validation LQI data set for the *toilet*.

Table 8. Room detection result for validation data of *Toilet*.

Room	Periods (min)	Percentage
Toilet	1∼418, 420, 422∼483, 485∼496, 499∼527, 535∼736	98.4%
D308	419, 421, 484, 497∼498, 528∼534	1.6%

5.5. Measured LQI Data and Detection Result for D307

D307 is the busiest room. Up to 16 students have their own desks, and may frequently enter and leave the room, and move around in the room. Figures 15 and 16 show the training LQI data set and the validation LQI data set for *D307*, respectively. A lot of fluctuations can be observed, where even *LQI2* fluctuated and sometimes lost connections, although the receiver was located in this room. Tables 9 and 10 show the room detection results for them, where *D308* and *Toilet* are incorrectly detected instead of *D307*. Fortunately, the room detection accuracy of *FILS15.4* reaches 99.5% for the training data set and 98.5% for the validation data set by the proposal.

Figure 15. Training LQI data set for *D307*.

Table 9. Room detection result for training data of *D307*.

Detected Room	Periods (min)	Percentage
D307	1∼598, 600∼941, 943∼1321, 1323∼1520, 1524∼1826, 1830∼2007, 2009∼2150	99.5%
D308	1828	0.1%
Toilet	599, 942, 1322, 1521∼1523, 1827, 1829, 2008	0.4%

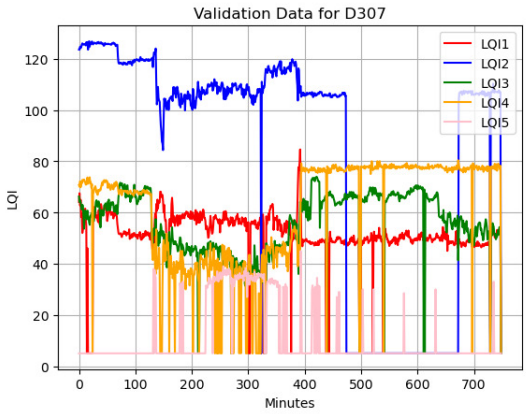

Figure 16. Validation LQI data set for *D307*.

Table 10. Room detection result for validation data of *D307*.

Room	Periods (min)	Percentage
D307	1∼323, 325∼497, 501∼540, 543∼611, 613, 615∼672, 674∼729, 731∼748	98.5%
Toilet	324, 498∼500, 541∼542, 612, 614, 673, 730, 749	1.5%

5.6. Measured LQI Data and Detection Result for D306

Then, Tables 5 and 6 show that the detection rate of *D306* is decreased the most from 99.2% for training data to 95.2% for validation data. Figures 17 and 18 show the training LQI data set and the validation LQI data set for *D306*, respectively. Tables 11 and 12 show the room detection results for them, where *Toilet* and *D308*, *D305* are incorrectly detected instead of *D306*.

In *D306*, four students have their own desks at the one side. Another side is used as the common meeting space by students. Therefore, the number of students staying in this room often changed, which can cause changes of the measured LQI data depending on the time.

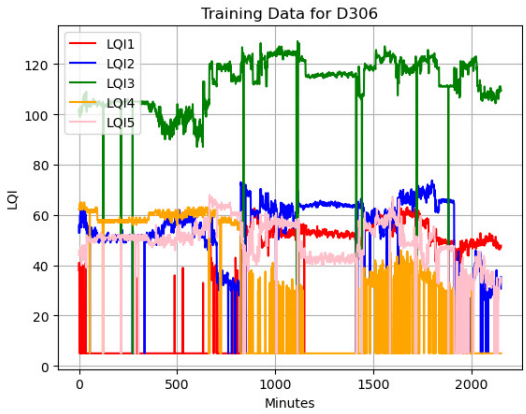

Figure 17. Training LQI data set for *D306*.

Table 11. Room detection result for training data of *D306*.

Room	Periods (min)	Percentage
D306	1∼124, 126∼214, 216∼273, 275∼838, 840∼1108, 1110, 1114, 1116∼1411, 1415∼1441, 1443∼1719, 1723∼1881, 1883∼2150	99.2%
Toilet	125, 215, 274, 839, 1109, 1111∼1113, 1115, 1412∼1414, 1721∼1722, 1882	0.7%
D308	1442, 1720	0.1%

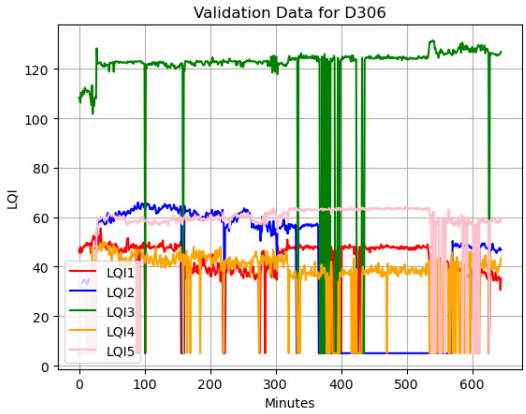

Figure 18. Validation LQI data set for *D306*.

Table 12. Room detection results for validation data of *D306*.

Room	Periods (min)	Percentage
D306	1∼101, 103∼159, 161∼334, 336∼368, 372, 375∼376, 378, 380, 383, 385∼391, 396, 398, 400∼424, 433, 437∼626, 628∼645	95.2%
Toilet	102, 160, 335, 369∼371, 373∼374, 377, 379, 381, 384, 392∼395, 397, 425∼432, 434∼436, 627	4.5%
D305	382, 399	0.3%

6. Evaluation over Time

In this section, we evaluate the robustness of the proposal by using the same fingerprints and the measured LQI data at the same floor on different periods.

6.1. Detection Result for LQI Data at Different Times

To verify the effectiveness of the optimized fingerprints by the proposal, we newly collected the LQI measured data for three days, five months after the previous one. Table 13 shows the detection results using the fingerprint values in Table 4 and also compares with the ANN model. Figure 19 shows the comparison of the detection results. It shows that the detection accuracy exceeds 98% for any room except for *Corridor* (94.5%) and *D307* (93.2%) by using the proposed method, where the accuracies for these rooms are sufficiently high. The ANN model also obtains high detection accuracy for each room, but the average detection accuracy is still lower than our proposed method. The score of new LQI data at three days was 94,070. Figure 20 shows CDF results for new data sets.

Table 13. Room detection results for new LQI data sets at different times.

Room	Accuracy (POT)	Accuracy (ANN)	$disF^{OK}$	$disF^{NG}$	Margin
RC	98.1%	97.1%	34.09	65.01	30.92
Corridor	94.5%	94.1%	38.46	46.11	7.65
D306	99.6%	99.2%	78.88	119.54	40.66
D307	93.2%	93.8%	32.81	43.16	10.35
D308	98.3%	95.9%	72.56	78.14	5.58
Toilet	99.2%	96.7%	42.11	53.8	11.69
D305	99.2%	98.3%	37.34	40.59	3.25
Average	97.4%	96.4%	48.04	63.76	15.72

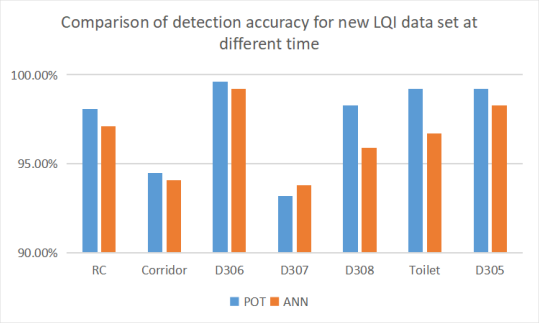

Figure 19. Comparison of detection accuracy for new LQI data sets at different times.

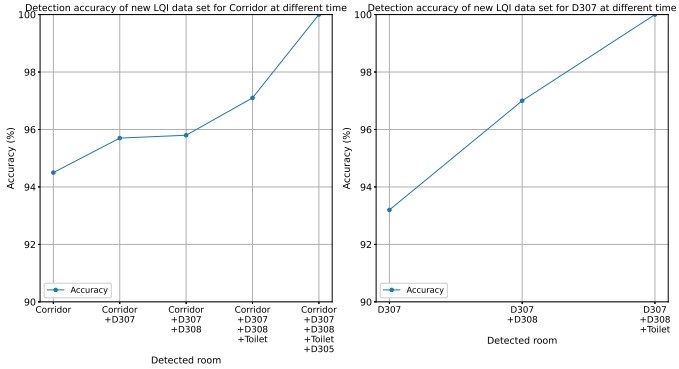

Figure 20. CDF of detection accuracy for new LQI data sets at different times.

6.2. Measured LQI Data and Detection Results for the Corridor

Here, we discuss why the accuracy decreased for the *corridor*. Figures 21 and 22 show the training LQI data set and the newly measured set for the *corridor*, and Tables 14 and 15 show the room detection results for them, respectively.

When the two graphs are compared, the LQI data are clearly different between them, including LQI5 at the receiver in *corridor*. In the *corridor*, people can often move. Thus, in the training LQI data set, a lot of fluctuations are observed, which suggests the frequent door opening/closing in the rooms where the receivers were allocated. However, in the newly measured set, the data are far from stable. This is because of few people at that time due to the *COVID-19* pandemic.

Figure 21. Training LQI data set for the *corridor*.

Table 14. Room detection result for training data of the *corridor*.

Room	Periods (min)	Percentage
Corridor	1∼88, 90∼95, 97∼104, 107∼111, 113∼205, 207∼421, 423∼540, 542∼547, 549∼556, 559∼563, 565∼806, 808∼1793, 1795∼2023, 2025∼2150	99.3%
D306	206	0.1%
D308	807, 2024	0.1%
Toilet	96, 105∼106, 548, 557∼558, 1794	0.3%
D305	89, 112, 422, 541, 564	0.2%

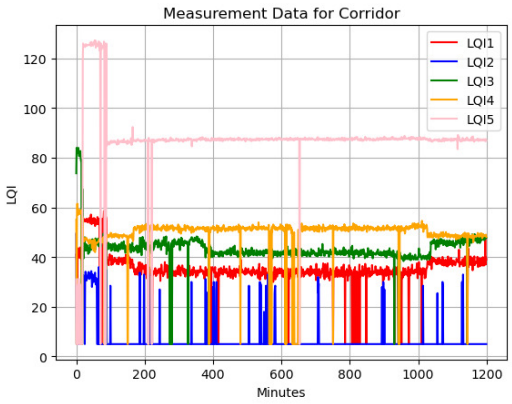

Figure 22. New LQI data set for *Corridor* at different time.

Table 15. Room detection results for new LQI data of the *corridor* at different time.

Room	Periods (min)	Percentage
Corridor	20∼71, 73∼83, 85, 89∼98, 100∼150, 153∼210, 214∼221, 223∼388, 391∼480, 482∼564, 567, 570∼571, 573∼611, 614, 616∼632, 634, 638, 650∼653, 655∼751, 753∼943, 947∼1119, 1121∼1144, 1146, 1148∼1196, 1198∼1200	94.5%
D307	3∼16	1.2%
D308	88	0.1%
Toilet	1∼2, 17∼19, 72, 84, 86∼87, 99, 211, 222, 654, 1120, 1147, 1197	1.3%
D305	151∼152, 212∼213, 389∼390, 481, 565∼566, 568∼569, 572, 612∼613, 615, 633, 635∼637, 639∼649, 752, 944∼946, 1145	2.9%

6.3. Measured LQI Data and Detection Result for D307

Next, we discuss why the accuracy decreased for *D307*. Figure 23 shows the newly measured LQI data set for *D307* and Table 16 shows room detection results.

When Figure 23 is compared with Figure 15, almost every LQI is different between them. In particular, the data of LQI5 was lost in Figure 23. Thus, it may be necessary to properly handle the low measured LQI data considering the disconnection between the transmitter and the receiver.

Figure 23. New LQI data set for *D307* at different times.

Table 16. Room detection results for new LQI data of *D307* at different times.

Room	Periods (min)	Percentage
D307	1∼216, 218∼220, 222∼223, 225∼226, 229, 233∼236, 238∼250, 254, 256∼259, 261∼273, 275∼276, 279∼280, 282∼283, 285∼292, 300∼301, 303, 305∼307, 314, 322, 324, 326∼328, 334, 336∼348, 354∼493, 497∼498, 502∼503, 507∼584, 586, 588, 590∼605, 607∼684, 686∼704, 706∼736, 739∼766, 768∼793, 797∼814, 816∼830, 832∼835, 837∼922, 924∼1000, 1002∼1061, 1063∼1189, 1191∼1200	93.2%
D308	217, 221, 224, 227∼228, 230∼232 237, 251∼253, 255, 260, 274, 277∼278, 281, 284, 304, 308, 329∼330, 494∼496, 499∼501, 504∼506, 585, 589, 606, 685, 705, 737∼738, 767, 815, 831, 836, 923, 1001, 1062	3.8%
Toilet	293∼299, 302, 309∼313, 315∼321, 323, 325, 331∼333, 335, 349∼353, 587, 794∼796, 1190	3%

7. Evaluation with Fluctuation Causes

In this section, we list the six causes for LQI data fluctuations; we conducted the experiments to evaluate the effects of them using the scenarios in Table 17. During the experiments, the transmitter was located at *D307-4* in Figure 3. For *door open/close*, the door of D307 was opened and closed. For *Wi-Fi*, the Wi-Fi interface of a smartphone was turned on and off in D307. For *human movement*, one, two, or three persons moved around in D307. For *transmitter direction*, the face of the transmitter was directed to eastward, westward, northward, southward, upward, and downward directions. For *transmitter movement*, the transmitter location was moved in the five rooms. For *transmitter height*, the height of the transmitter from the floor was changed.

We show the results by each transmitter height as follows. Figures 24–27 show the measured LQI data, when the transmitter height was 0.5 m, 1 m, 1.5 m, and 1.8 m, respectively. Tables 18–21 summarize the average and standard deviation (SD) of the LQI data and the room detection accuracy of the proposed *FILS15.4* for each transmitter height. The same fingerprint values given in Section 5.3.1 in the previous submission were adopted for the room detection.

These results indicate that the measured LQI data are frequently fluctuating at any case of the six fluctuation causes. Nevertheless, the room detection accuracy of *FILS15.4* is sufficiently high for any case of the fluctuation causes when the transmitter location is fixed (no *transmitter movement*). Even for *transmitter movement*, the accuracy reached 94% when the transmitter height was 1.8 m. As the transmitter height increases, the obstacles between the transmitter and the receivers are reduced. Thus, stronger and more stable signals can be detected at the receivers, which reduces the LQI data fluctuations and improves the detection accuracy.

Table 17. Experimental scenarios for LQI fluctuation causes.

Fluctuation Cause	Experiment Scenario
door open/close	• 0–20 min: open • 20–40 min: close • 40–60 min: frequently open/close
Wi-Fi on/off	• 0–30 min: on • 30–35 min: off • 35–60 min: on
human movement	• 0–20 min: three persons • 20–40 min: two persons • 40–60 min: one person
transmitter direction	• 0–10 min: east • 10–20 min: west • 20–30 min: north • 30–40 min: south • 40–50 min: up • 50–60 min: down
transmitter movement	• 0–10 min: D306 • 10–20 min: Refresh Corner • 20–30 min: D307 • 30–40 min: Corridor • 40–50 min: D308
transmitter height	• 0.5 m • 1 m • 1.5 m • 1.8 m

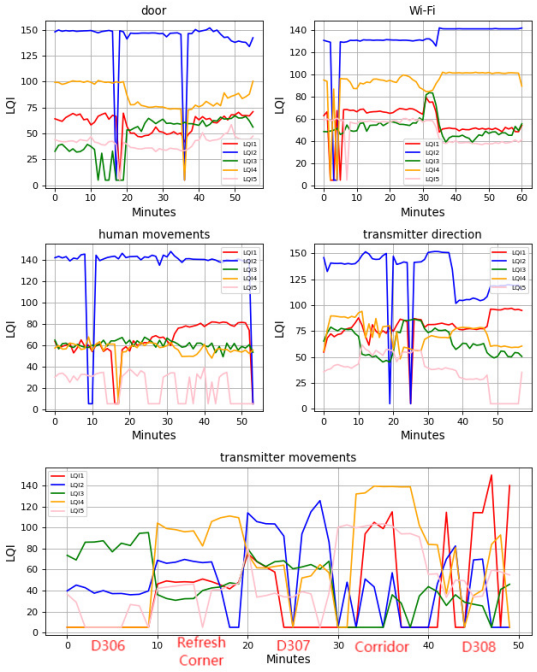

Figure 24. Fluctuation LQI data at 0.5 m.

Table 18. Fluctuation LQI data summary and detection accuracy at 0.5 m.

Fluctuation Cause	Value	LQI1	LQI2	LQI3	LQI4	LQI5	Accuracy
door open/close	AVE SD	59.24 10.89	141.24 26.71	48.71 18.93	85.29 15.33	40.46 7.1	96.4%
Wi-Fi on/off	AVE SD	57.56 14.88	130.85 23.96	52.14 9.19	93.3 17.2	49.03 11.22	96.7%
human movement	AVE SD	64.41 17.46	134.01 31.67	60.54 3.68	56.05 8.22	21.59 13.56	96.2%
transmitter direction	AVE SD	79.63 13.42	128.18 28.63	65 12.69	71.87 11.76	37.31 16.73	96.6%
transmitter movement	AVE SD	38.36 43.16	49.09 35.58	46.71 27.04	64.82 47.5	47.96 30.65	82%

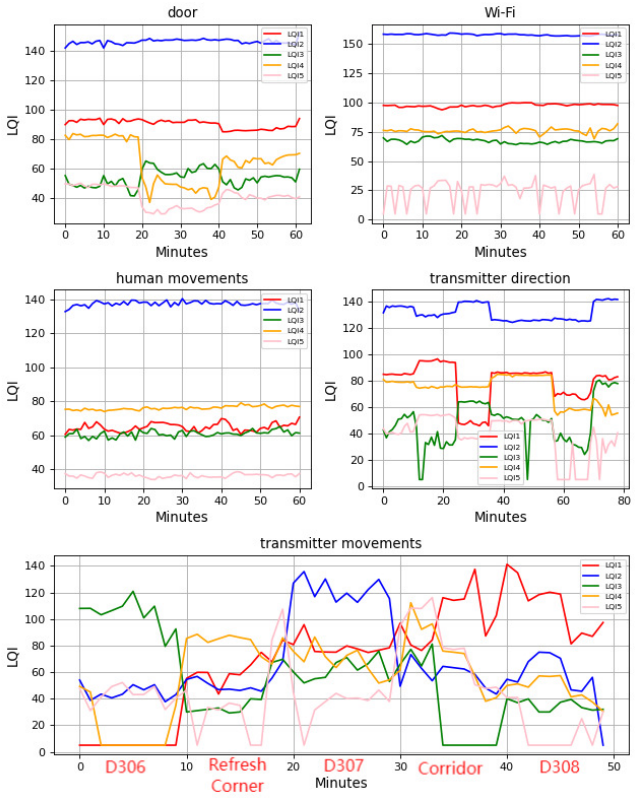

Figure 25. Fluctuation LQI data at 1 m.

Table 19. Fluctuation LQI data summary and detection accuracy at 1 m.

Fluctuation Cause	Value	LQI1	LQI2	LQI3	LQI4	LQI5	Accuracy
door open/close	AVE SD	90.3 2.97	146.41 1.6	53.39 5.59	64.67 14.71	40.44 6.89	100%
Wi-Fi on/off	AVE SD	97.27 1.31	157.27 0.67	67.05 1.87	75.73 2.0	24.3 10.09	100%
human movement	AVE SD	64.89 2.38	137.53 1.45	61.0 1.88	76.21 1.12	36.36 1.13	100%
transmitter direction	AVE SD	78.5 14.84	131.35 6.25	48.13 17.02	73.16 10.27	38.88 15.48	100%
transmitter movement	AVE SD	71.55 39.86	66.34 30.54	54.53 32.21	57.31 27.81	43.18 29.29	82%

Table 20. Fluctuation LQI data summary and detection accuracy at 1.5 m.

Fluctuation Cause	Value	LQI1	LQI2	LQI3	LQI4	LQI5	Accuracy
door open/close	AVE SD	85.63 25.01	126.69 33.53	50.25 8.43	70.37 23.51	28.8 10.63	93.1%
Wi-Fi on/off	AVE SD	85.21 14.85	136.65 24.23	70.4 2.8	69.62 9.5	47.8 1.06	96.8%
human movement	AVE SD	72.89 9.51	122.55 16.38	73.04 1.25	48.04 9.0	7.79 8.06	98.1%
transmitter direction	AVE SD	78.11 24.08	116.35 30.07	68.27 20.79	64.08 12.87	42.19 9.53	94.7%
transmitter movement	AVE SD	81.74 31.28	71.03 23.79	65.3 30.57	65.25 24.85	45.46 15.89	88%

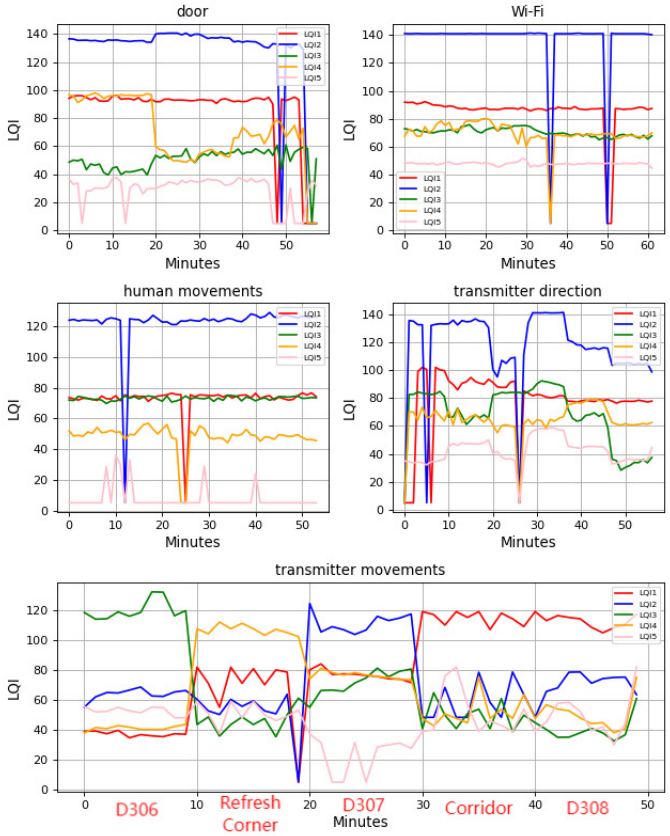

Figure 26. Fluctuation LQI data at 1.5 m.

Table 21. Fluctuation LQI data summary and detection accuracy at 1.8 m.

Fluctuation Cause	Value	LQI1	LQI2	LQI3	LQI4	LQI5	Accuracy
door open/close	AVE SD	72.02 7.03	150.97 10.27	74.91 5.52	90.01 7.42	51.42 6.3	100%
Wi-Fi on/off	AVE SD	92.03 1.02	114.56 3.2	74.37 1.79	82.61 1.08	44.53 1.45	100%
human movement	AVE SD	95.28 2.73	112.67 5.19	77.65 2.39	83.63 1.23	41.81 2.82	100%
transmitter direction	AVE SD	84.09 14.88	120.46 18.24	88.66 19.51	74.95 15.14	45.62 11.86	100%
transmitter movement	AVE SD	74.79 26.96	75.47 25.81	69.73 32.11	67.42 27.85	62.31 24.37	94%

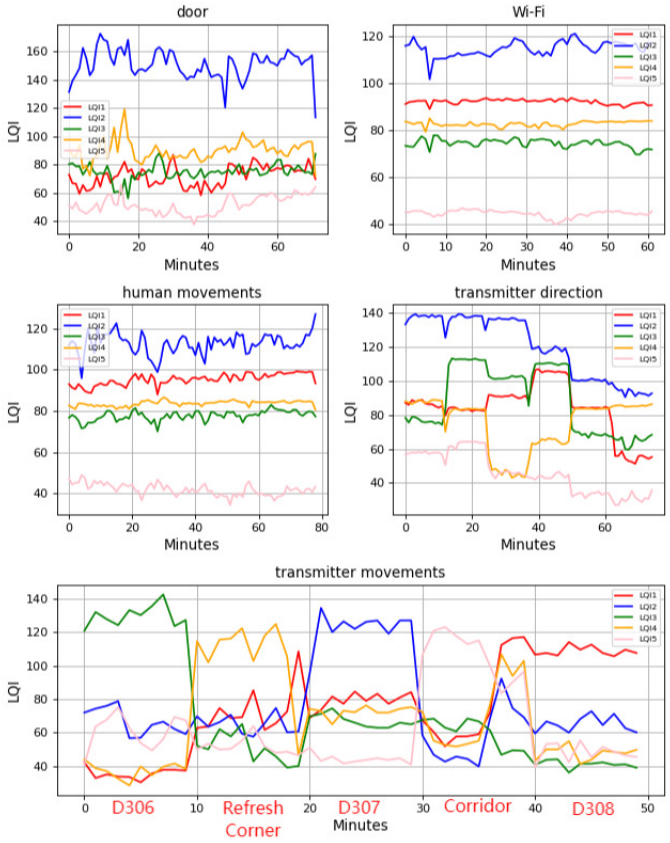

Figure 27. Fluctuation LQI data at 1.8 m.

8. Discussion

The results in Tables 5, 6 and 13 using the static transmitter show that the proposed fingerprint optimization method sufficiently improves the room detection accuracy of *FILS15.4* by increasing the number of fingerprints in one room and optimizing their values automatically, when the user stays in a room for a while. Table 4 indicates that the number of fingerprints for each room increased to two or three except for *D306* by this method. Particularly, it became three for *corridor* and *toilet* where the detection accuracy was low before applying the method as in Table 3.

Moreover, the results in Table 21 show that the high detection accuracy can be maintained under influences by various LQI fluctuation causes, including the room door open/close, the Wi-Fi signal on/off, human movements around the transmitter, the change of the transmitter face direction, movements of the transmitter with the user, when the transmitter is attached to the user at 1.8 m of height. It should be noted that the same optimized set of the fingerprints for the static transmitter were used here. Thus, the effectiveness of the proposal is confirmed.

However, our experiments in this paper were conducted under rather impractical situations. The transmitter was placed alone at a location for a long time, or was moved around in a short time with the user. The detection accuracy of *FILS15.4* under practical situations needs to be evaluated, where the user may keep the transmitter for whole day and may move from one room to another occasionally. In future works, we will design and conduct experiments under practical situations.

Moreover, the considered LQI fluctuation causes in our experiments may still be limited. LQI fluctuations may be different due to the time, weather, and season. In future works, we will evaluate the detection accuracies of *FILS15.4* at different weather conditions, times, days, and seasons.

9. Related Works

In this section, we discuss related works in the literature.

In [14], Youssefa et al. proposed a WLAN location determination system by clustering the access point (AP) signal strength distribution and determine the user's location based on Bayes' probabilistic approach. It identified that the wireless channel varies due to several causes, namely different signal strength samples and AP-to-user distance variations. Those causes of variations were included in their clustering algorithm to determine the user's location. The testbed system achieved 90% of detection accuracy.

In [15], Sen et al. found the evidence that channel responses from multiple orthogonal frequency–division multiplexing (OFDM) subcarriers can be a promising location signature. While these signatures certainly vary over time and environmental mobility, they noticed that the core structure preserves certain properties that are amenable to the localization. They evaluated the system in a real busy engineering building and demonstrated localization accuracies in the granularity of 1×1 m boxes, called "spots". The results from 100 spots showed that their proposal was able to localize a user to the correct spot with the 89% of the average accuracy. Less than 6% of its inaccuracy falsely detected a location where the user was not present (false positive).

In [16], Turner et al. proposed the use of a *wireless sensor network (WSN)* to investigate the effects caused by human movements on *(RSSI)*. They conducted measurements in real environments. The results showed that slow human movements reduced the effects and fast ones slightly decreased them. They did not study how sensor heights affected signal fluctuations.

In [17], Hamdoun et al. proposed an indoor localization method by using multiple antennas in wireless sensor networks. They used the multilateration as well as the trilateration algorithms, based on the RSSI values to estimate the target position. They considered three systems namely, the single antenna system (single input single output, SISO), the multiple receive antenna system (single input multiple output, SIMO), and the multiple transmit antenna system (multiple input single output, MISO). The average localization accuracy error is improved when the average RSSI is calculated from multiple antennas. The performance improvement was increased to 30% and 50% when using two and four antennas, respectively. The performance accuracy improved considerably while increasing the number of antennas. Thus, MIMO performed as the best system, followed by SIMO and MISO with similar performance, and SISO with the largest localization error. Moreover, the multilateration was shown to perform better than the trilateration algorithm.

In [18], Luoh et al. proposed a *ZigBee*-based indoor localization system using the *radial basis function network (RBFN)* with the fingerprinting method. They conducted measurements in real environments where human effects were not evaluated in experiments.

In [19], Koweerawong et al. proposed a method to estimate the *RSS* fingerprint of a specific location from a set of neighboring remeasured *RSS* fingerprints called "feedbacks". The method searches for new feedback, requires old *RSS* fingerprints in the cut-off area, and applies the plane interpolation to calculate the new *RSS* fingerprint for a specific location. However, the detection accuracy was not improved. The proposal was evaluated only in simulations.

In [20], Ferdews et al. proposed a new distributed and time-bound localization algorithm based on the multidimensional scaling (MDS) method in a wireless sensor network (WSN) called the D-MDS localization time algorithm. They compared the proposed algorithm to the existing algorithm based on the well-known trilateration method. In experiments, they implemented D-MDS by using a MATLAB simulator and evaluated the proposed algorithm by comparing it to the time-bound localization algorithm based on the trilateration method. The simulation results showed their proposed algorithm was faster to check the relative localization ability of the network compared with the trilateration algorithm in terms of time complexity.

In [21], Torteeka et al. presented a K-nearest neighbor (K-NN) method based on the crisp set theory to select the nearest Euclidean distance. Their algorithm showed better performances than a simple K-NN method, only in simulations, not in real environments.

In [22], Aomumpai et al. proposed a technique to optimize the placements of the reference nodes to improve the detection accuracy. Their results showed 90% precision as the detection accuracy through only simulations.

In [23], Chapre et al. proposed Wi-Fi-based fingerprinting using the fine-grained information of a physical layer known as channel state information (CSI). It exploited the frequency and spatial diversity of the multiple-input multiple-output (MIMO) system and generated a complex location signature by including the amplitude and phase information of all sub-carriers. The testbed was evaluated in two rooms with different sizes. The smaller room was used for the static environment, whereas the bigger room was for the dynamic one. The deterministic k-nearest neighbor (kNN) and the probabilistic Bayes' rule were used as their localization algorithms. In their investigation, the static and the dynamic environment have different amplitude and phase variance characteristics. The CSI exhibited less phase fluctuations when it was static, while significant variations of phases were found in dynamic conditions. The proposal achieved the maximum accuracy of 0.98 and 0.31 m using the deterministic k-nearest neighbor algorithm in static and dynamic environments, respectively.

In [24], Hamdoun et al. proposed a comparative study of RSSI-based localization algorithms using spatial diversity in wireless sensor networks (WSNs). They considered different kinds of single/multiple antenna systems: single input single output (SISO) system, single input multiple output (SIMO) system, multiple input single output (MISO) system, and multiple input multiple output (MIMO) system. They focused on the well-known trilateration and multilateration localization algorithms to evaluate and compare different antenna systems. In addition, exploiting the spatial diversity by using multiple antenna systems can significantly improve the accuracy of the location estimation. They used three diversity-combining techniques at the receiver in their experiments: maximal ratio combiner (MRC), equal gain combining (EGC), and selection combining (SC). The results have shown that the localization performance in terms of position accuracy was improved when using multiple antennas. An improvement in the performance of about 30% was achieved with four antenna usages compared to two antennas. Specifically, using multiple antennas on both sides presented better performances than using multiple antennas only at the transmitting or receiving side.

In [25], Prieto et al. assessed the proposed framework with conventional Wi-Fi devices in comparison to conventional implementations. They conducted measurements in real environments. However, the proposed framework needs too many fingerprints for the high localization accuracy.

In [26], Ma et al. proposed a *Wi-Fi*-based indoor positioning algorithm using the weighted fusion. The offline acquisition process selects optimal parameters to complete the signal acquisitions and forms the database of fingerprints by the error classifications. The online positioning process uses the pre-match method to select the candidate fingerprints to shorten the positioning time. However, the fingerprints are updated manually. The proposal was evaluated only in simulations.

In [27], Vasisht et al. proposed *Chronos*, a system that enables a single Wi-Fi access point to localize clients to within tens of centimeters. They conducted experiments in a two-bedroom apartment with four occupants, with dimensions of the experiment room at 13×9 m. The results showed the average detection accuracy was 94.3% at the room level and the average of the distance error was 14.1 cm.

In [28], Alshami et al. studied how the distance between a smartphone and an access point caused *RSS* fluctuations. They evaluated the proposal in real environments.

In [29], Wang et al. studied fingerprinting-based indoor localization in commodity 5-GHz Wi-Fi networks and proposed a system *BiLoc*, which used bi-modality deep learning for localization in the indoor environment. In their experiment, firstly, they used a channel

state information (CSI) data built fingerprint at offline stage and detected the location of the user in their lab at the online stage. The results show the average of distance error was 1.5 m.

In [30], Bernas et al. introduced a method that improves localization accuracy of the signal strength fingerprinting approach. In the proposed method, the entire localization area was divided into several regions by clustering the fingerprint database. For each region, a sample of the received signal strength was determined and a dedicated artificial neural network (ANN) was trained by using only the fingerprints that belonged to this region (cluster).

In [31], Uradzinski et al. proposed the nearest neighbor and Bayesian methods using *IEEE 802.15.4 protocol* devices, which promised less than or equal to the 0.81 m accuracy. They first collected data and created a fingerprint database. Next, they used the nearest-neighbor and Bayesian methods to detect the indoor positioning of each person. However, they did not evaluate the proposal in multiple rooms and considered human effects in experiments.

In [32], Saber et al. proposed and implemented a new mechanism for geographic routing in wireless sensor networks (WSNs). The proposed mechanism relied on a weighted centroid localization technique, where the positions of unknown nodes were calculated using the fuzzy logic method. They proposed a fuzzy localization algorithm that used flow measurement through a wireless channel to compute the distance separating the anchor and the sensor nodes. They were based on the centroid algorithm that calculated the position of unknown nodes using the fuzzy Mamdani and Sugeno inference system for increasing the accuracy of estimated positions. Once the localization algorithm detected the location of nodes with an unknown position, the proposed mechanism effectively selected the next-elected cluster head (CH) to reduce the energy dissipation of sensor nodes. Thus, it extended the network lifetime. Their method had two advantages: the first was to minimize the position error of nodes and reduce the error localization average. The second was to increase the number of packets transmitted to the next hop of CH based on the localization algorithm. The obtained simulation results showed that the Sugeno technique achieved a better performance than the centroid and Mamdani techniques together. Using the Sugeno method, they had an average location error equal to 0.3 m and the simple centroid was 0.8 m. The proposed mechanism outperforms the existing solutions in terms of energy consumption, execution time (localization time), and localization error, similar to the number of packets transmitted to the base station.

In [33], Omer et al. proposed the indoor localization system using the UHF radio frequency identification (RFID). Unfortunately, it needs to allocate a lot of reader antennas for use in a conventional field with several rooms; their label just attached on the coat or other objects, they did not attach on the human body.

In [34], Ashraf et al. showed a similar indoor localization approach that turns smartphone built-in sensors to good account. They took advantage of the magnetic field strength fingerprinting approach to localize a pedestrian indoors. Their aim was to solve the problem of device dependence by devising an approach that could perform localization using various smartphones in a similar fashion. They conducted experiments using Samsung Galaxy S8 and LG G6 for five different buildings with different dimensions at Yeungnam University, Republic of Korea. The proposed approach can potentially localize a pedestrian within 1.21 m at 50% and within 1.93 m at 75%. The performance of the proposed approach was compared with the K nearest neighbor (KNN) for evaluation. The proposed approach outperforms the KNN.

In [35], Setiabudi et al. proposed a method using Bluetooth low energy (BLE) to estimate the position of a dynamic user based on fingerprinting with the weighted sum of five nearest reference points using the extended Kalman filter. Unfortunately, even though they conducted measurements in a real environment, the proposed method needs to allocate a lot of transmitters in the target field, and the positioning accuracy is not sufficient.

In [36], Ashraf et al. presented a comprehensive review of the approaches that made use of data from one or more sensors to estimate the user's indoor location. By analyzing the approaches leveraged on smartphone sensors, the review discusses the associated challenges of such approaches and points out the areas that need considerable research to overcome their limitations.

In [37], Njima et al. proposed generative adversarial networks for the RSSI data augmentation to generate fake RSSI data based on a small set of real collected labeled data. The developed model utilizes the semi-supervised learning in order to predict the pseudo-labels of the generated RSSI. Their extensive numerical experiments show that the proposed data augmentation and selection scheme leads to the localization accuracy improvement of 21.69% for simulated data and 15.36% in the experiment data.

In [38], Fahmy et al. proposed a *Wi-Fi*-based indoor localization system named *MonoFi*. It relied on the received signal strength from a single access point and trained the recurrent neural network with sequences of signal measurements. They conducted measurements in real environments. The results show that the median localization error was 0.80 m in their experiments.

In [39], Jiang et al. proposed a fingerprint-based indoor localization method named the *fingerprint feature extraction (FPFE)*. It uses *Wi-Fi* signals to detect human locations. The average detection error in experiments using one room in real environments was 0.68 m. They did not conduct experiments in multiple rooms.

In [40], Ezhumalai et al. proposed an *RSS* measurement technique named *(IRSSMT)* to minimize the error of *RSS* observations by using several selected *RSS* and its median values, and the *strongest access point (SAP)* information-based clustering technique that groups the *reference points (RPs)* using the *SAP* similarity.

In this paper, we evaluated the proposal through experiments in real indoor environments with multiple rooms where human effects and other signal fluctuation causes were considered.

In previous works, they used Wi-Fi signals for fingerprints. However, the devices consume a lot of energy, are too large and heavy to always be carried during the localization, and can be expensive. On the other hand, in this study, we used IEEE 802.15.4-based *Twelite 2525* transmitters from *Mono Wireless*. They have advantages over Wi-Fi-based devices, e.g., small sizes (13.97 $\times$ 13.97 $\times$ 2.5 mm), are lightweight 0.93 g, have long battery lives with coin batteries, at a low cost (USD 30), no user software downloading, and no user setup.

10. Conclusions

This paper presents the *parameter optimization method*, to find the proper fingerprints in a *fingerprint-based indoor localization system using IEEE802.15.4 (FILS15.4)*. The method iteratively changes fingerprint values to maximize the newly defined *score function* to evaluate the room detection accuracy of the system. Moreover, it automatically increases the number of fingerprints for a room if the accuracy is insufficient.

For evaluations, the proposed method was extensively applied to the measured LQI data using the *FILS15.4* testbed system in the no. 2 Engineering Building at Okayama University. The *validation* results with the static transmitter show that the method improves the average room detection accuracy at higher than 97% by automatically increasing the number of fingerprints and optimizing their values. Moreover, the results with the transmitter under LQI fluctuation causes also showed high accuracy using the same set of fingerprints. Thus, the effectiveness of the proposal was confirmed.

In future works, we will evaluate the detection accuracy of *FILS15.4* under practical situations where the user may keep the transmitter for whole days and occasionally move from one room to another. Moreover, we will evaluate it at different weather conditions, times, days, and seasons for further LQI fluctuation causes.

Author Contributions: Conceptualization, Y.H. and N.F.; methodology, Y.H.; software, Y.H. and P.P.; validation, K.H., M.K. and K.K. All authors have read and agreed to the published version of the manuscript.

Funding: This research received no external funding.

Institutional Review Board Statement: Not applicable.

Informed Consent Statement: Not applicable.

Data Availability Statement: Not applicable.

Acknowledgments: The authors thank the reviewers for their thorough reading and helpful comments.

Conflicts of Interest: The authors declare no conflict of interest.

References

1. Curran, K.; Furey, E.; Lunney, T.; Santos, J.; Woods, D.; McCaughey, A. An Evaluation of Indoor Location Determination Technologies. *J. Loc. Base. Serv.* **2011**, *5*, 61–78. [CrossRef]
2. Kunhoth, J.; Karkar, A.; Al-Maadeed, S.; Al-Ali, A. Indoor Positioning and Wayfinding Systems: A Survey. *Hum.-Cent. Comput. Inf. Sci.* **2020**, *10*, 18. [CrossRef]
3. Al-Ammar, M.A.; Alhadhrami, S.; Al-Salman, A.; Alarifi, A.; Al-Khalifa, H.S.; Alnafessah, A.; Alsaleh, M. Comparative Survey of Indoor Positioning Technologies, Techniques, and Algorithms. In Proceedings of the International Conference on Cyberworlds, Cantabria, Spain, 6–8 October 2014; pp. 245–252.
4. Brena, R.F.; Garcia-Vazquez, J.P.; Galvan-Tejada, C.E.; Munoz-Rodriguez, D.; Vargas-Rosales, C.; Fangmeyer, J. Evolution of Indoor Positioning Technologies: A Survey. *J. Sens.* **2017**, *1*, 1–21. [CrossRef]
5. Davidson, P.; Piche, R. A Survey of Selected Indoor Positioning Methods for Smartphones. *IEEE Commun. Surv. Tutor.* **2016**, *19*, 1347–1370. [CrossRef]
6. Molina, B.; Olivares, E.; Palau, C.E.; Esteve, M. A Multimodal Fingerprint-Based Indoor Positioning System for Airports. *IEEE Access* **2018**, *6*, 10092–10106. [CrossRef]
7. Puspitaningayu, P.; Hamazaki, K.; Funabiki, N.; Htet, H.; Kuribayashi, M. *An Implementation of Fingerprint-Based Indoor Positioning System Using IEEE 802.15.4*; IEICE Tech. Report, LOIS2020-28; IEICE: Tokyo, Japan, January 2021; pp. 33–38.
8. Yuanzhi, H.; Puspitaningayu, P.; Funabiki, N. A Parameter Optimization Method for Fingerprint-Based Indoor Localization System Using IEEE 802.15. 4 Devices. In Proceedings of the International Conference on Computer Communication and the Internet, Nagoya, Japan, 25–27 June 2021; pp. 136–140.
9. Mono Wireless. Mono Wireless Product Information. Available online: https://mono-wireless.com/jp/products/index.html (accessed on 10 May 2021).
10. Funabiki, N.; Taniguchi, C.; Lwin, K.S.; Zaw, K.K. ; Kao, W.C. A Parameter Optimization Tool and Its Application to Throughput Estimation Model for Wireless LAN. *Adv. Intell. Syst. Comput.* **2017**, *611*, 701–710.
11. Mrindoko, N.R.; Minga, L.M. A Comparison Review of Indoor Positioning Techniques. *Int. J. Comp.* **2016**, *1*, 42–49.
12. Choi, M.S.; Beakcheol, J. An Accurate Fingerprinting Based Indoor Positioning Algorithm. *Int. J. Appl. Eng. Res.* **2017**, *12*, 86–90.
13. MQTT The Standard for IoT Messaging. Available online: https://mqtt.org/ (accessed on 10 May 2021).
14. Youssef, M.; Agrawala, A. The Horus WLAN Location Determination System. In Proceedings of the International Conference on Mobile Systems, Cologne, Germany, 6–8 June 2005; pp. 205–218.
15. Sen, S.; Radunovic, B.; Choudhury, R.; Minka, T. You Are Facing the Mona Lisa: Spot Localization Using PHY Layer Information. In Proceedings of the 10th International Conference on Mobile Systems, Applications, and Services, Windermere, UK, 25–29 June 2012; pp. 183–196.
16. Turner, J.S.C.; Ramli, M.F.; Kamarudin, L.M.; Zakaria, A.; Shakaff, A.Y.M.; Ndzi, D.L.; Nor, C.M.; Hassan, N.; Mamduh, S.M. The Study of Human Movement Effect on Signal Strength for Indoor WSN Deployment. In Proceedings of IEEE Conference on Wireless Sensor, Kuching, Malaysia, 2–4 December 2013; pp. 30–35.
17. Hamdoun, S.; Rachedi, A.; Benslimane, A. Comparative Analysis of RSSI-Based Indoor Localization When Using Multiple Antennas in Wireless Sensor Networks. In Proceedings of the 2013 International Conference on Selected topics in mobile and wireless networking (MoWNeT), Montreal, QC, Canada, 19–21 August 2013; pp. 146–151. [CrossRef]
18. Luoh, L. ZigBee-Based Intelligent Indoor Positioning System Soft Computing. *Soft Comput.* **2013**, *18*, 443–456. [CrossRef]
19. Koweerawong, C.; Wipusitwarakun, K.; Kaemarungsi, K. Indoor Localization Improvement via Adaptive RSS Fingerprinting Database. In Proceedings of the International Conference on Information Networking, Bangkok, Thailand, 28–30 January 2013; pp. 412–416.
20. Tlili, F.; Rachedi, A.; Benslimane, A. Time-Bounded Localization Algorithm Based on Distributed Multidimensional Scaling for Wireless Sensor Networks. In Proceedings of the 2014 IEEE International Conference on Communications (ICC), Sydney, Australia, 10–14 June 2014; pp. 233–238.

21. Torteeka, P.; Chundi, X. Indoor Positioning Based on Wi-Fi Fingerprint Technique Using Fuzzy K-Nearest Neighbor. In Proceedings of the 11th International Bhurban Conference on Applied Sciences & Technology, Islamabad, Pakistan, 14–18 January 2014; pp. 461–465.
22. Aomumpai, S.; Kondee, K. Optimal Placement of Reference Nodes for Wireless Indoor Positioning Systems. In Proceedings of the 11th International Conference on Electrical Engineering/Electronics, Computer, Telecommunications and Information Technology, Nakhon Ratchasima, Thailand, 14–17 May 2014; pp. 1–6.
23. Chapre, Y.; Ignjatovic, A.; Seneviratne, A; Jha, S. CSI-MIMO: An Efficient Wi-Fi Fingerprinting Using Channel State Information with MIMO. *Pervasive Mob. Comput.* **2015**, *23*, 89–103. [CrossRef]
24. Hamdoun, S.; Rachedi, A.; Benslimane, A. RSSI-Based Localisation Algorithms Using Spatial Diversity in Wireless Sensor Networks. *Int. J. Hoc Ubiquitous Comput.* **2015**, *19*, 157–167. [CrossRef]
25. Prieto, J.; De Paz, J.F.; Villarrubia, G.; Bajo, J.; Corchado, J.M. Unified Fingerprinting/Ranging Localization for E-Healthcare Systems. *Ambient. Intel. Soft. Appl.* **2015**, *376*, 223–231.
26. Ma, R.; Guo, Q.; Hu, C.; Xue, J. An Improved Wi-Fi Indoor Positioning Algorithm by Weighted Fusion. *Sensors* **2015**, *15*, 21824–21843. [CrossRef] [PubMed]
27. Vasisht, D.; Kumar, S.; Katabi, D. Decimeter-Level Localization with A Single WiFi Access Point. In Proceedings of the 13th USENIX Symposium on Networked Systems Design and Implementation, Santa Clara, CA, USA, 16–18 March 2016; pp. 165–178.
28. Alshami, I.H.; Ahmad, N.A.; Sahibuddin, S. The Effect of People Presence on WLAN RSS is Governed by Influence Distance. In Proceedings of the 3rd International Conference on Computer and Information Sciences, Kuala Lumpur, Malaysia, 15–17 August 2016; pp. 197–220.
29. Wang, X.; Gao, L.; Mao, S. BiLoc: Bi-Modal Deep Learning for Indoor Localization with Commodity 5 GHz WiFi. *IEEE Access* **2017**, *5*, 4209–4220. [CrossRef]
30. Bernas, M.; Płaczek, B. Fully Connected Neural Networks Ensemble with Signal Strength Clustering for Indoor Localization in Wireless Sensor Networks. *Int. J. Distrib. Sens. Netw.* **2017**, *45*, 403242–403252. [CrossRef]
31. Uradzinski, M.; Guo, H.; Liu, X.; Yu, M. Advanced Indoor Positioning Using Zigbee Wireless Technology. *Wirel. Pers. Commun.* **2017**, *97*, 6509–6518. [CrossRef]
32. Amri, S.; Khelifi, F.; Bradai, A.; Rachedi, A.; Kaddachi, M.L.; Atri, M. A New Fuzzy Logic Based Node Localization Mechanism for Wireless Sensor Networks. *Future Gener. Comput. Syst.* **2019**, *93*, 799–813. [CrossRef]
33. Omer, M.; Ran, Y.; Tian, G.Y. Indoor Localization Systems for Passive UHF RFID Tag Based on RSSI Radio Map Database. *Prog. Electron. Res.* **2019**, *77*, 51–60. [CrossRef]
34. Ashraf, I.; Hur, S.; Shafiq, M.; Kumari, S.; Park, Y. GUIDE: Smartphone Sensors-Based Pedestrian Indoor Localization with Heterogeneous Devices. *Int. J. Commun. Syst.* **2019**, *32*, e4062. [CrossRef]
35. Setiabudi, C.A.; Riady, A.; Kusuma, G.P. Indoor Positioning System Using BLE for Tracking Dynamic User Positions. *Int. J. Emer. Trend. Eng. Res.* **2020**, *8*, 455–463. [CrossRef]
36. Ashraf, I.; Hur, S.; Park, Y. Smartphone Sensor Based Indoor Positioning: Current Status, Opportunities, and Future Challenges. *Electronics* **2020**, *9*, 891. [CrossRef]
37. Njima, W.; Chafii, M. Indoor Localization Using Data Augmentation via Selective Generative Adversarial Networks. *IEEE Access* **2021**, *9*, 98337–98347. [CrossRef]
38. Fahmy, I.; Ayman, S.; Rizk, H.; Youssef, M. MonoFi: Efficient Indoor Localization Based on Single Radio Source and Minimal Fingerprinting. In Proceedings of the 29th International Conference on Advances in Geographic Information, Beijing, China, 2–5 November 2021; pp. 674–675.
39. Jiang, J.R.; Subakti, H.; Liang, H.S. Fingerprint Feature Extraction for Indoor Localization. *Sensors* **2021**, *21*, 5434. [CrossRef]
40. Ezhumalai, B.; Song, M.; Park, K. An Efficient Indoor Positioning Method Based on Wi-Fi RSS Fingerprint and Classification Algorithm. *Sensors* **2021**, *21*, 3418. [CrossRef] [PubMed]